

Optical bistability in finite-size nonlinear bidimensional photonic crystals doped by a microcavity

E. Centeno and D. Felbacq

LASMEA UMR-CNRS 6602, Complexe des C ezeaux, 63177 Aubi ere Cedex, France

(Received 10 July 2000)

We numerically demonstrate the existence of optical bistability in a finite-size nonlinear bidimensional photonic crystal doped by a microcavity. The numerical results are obtained by a rigorous theory of diffraction. We provide a theoretical model allowing to predict and explain the bistability phenomena from the resonances of the structure.

Numerous studies have been devoted to photonic crystals, i.e., periodic dielectric devices, made of linear materials.¹ These structures could allow us to obtain full gaps, to realize laser microcavities with a very high efficiency, multiplexers, or directive antennas.²⁻⁶ However, the analogy between semiconductors and linear photonic crystals cannot be pushed too far inasmuch as photons, being not submitted to Coulomb interaction, are not as easily controlled as electrons are. In particular, linear photonic crystals are not easily tunable. For these reasons, it seems natural to turn to photonic crystals made of nonlinear media. Some explicit computations have been made in case of one-dimensional (1D) nonlinear photonic crystals⁷⁻¹⁰ (note that these are just Bragg mirrors, and that bistability is known to occur in nonlinear Fabry-Perot resonators). In particular a very interesting physical phenomenon, that of ‘‘gap soliton,’’ has been demonstrated.¹¹⁻¹³ The subject of two- and three-dimensional solitons has also been dealt with by John and Ak ozbek with some approximations^{14,15} (media with small-contrast, slowly varying envelope approximation, etc.). Finally, bistability near a bandedge has been numerically investigated.¹⁶⁻¹⁸ However, all these studies, apart from in the case of 1D structures, deal with the four-wave approximation and use the Bloch-waves decomposition. For our part, we are interested in the computation of the energy transmitted through a finite-size nonlinear photonic crystal, so as to be as close as possible to an experimental situation. The crystal is doped with a microcavity (we have removed a rod at the center of the crystal). In the linear theory, such a microcavity generates a deep acceptor mode. We demonstrate that this property may be used, in the case of a nonlinear material, to induce optical switching and bistability in the transmission ratio.

We use the doped crystal depicted in Fig. 1, made of 26 infinitely long parallel rods made of a material with $\chi^{(3)}$ nonlinearity. An *s*-polarized plane-wave impinges on the structure from the upper face and the transmission coefficient *T* is defined as the ratio between the flux of the Poynting vector of the total field collected on a segment situated below the crystal to the flux of the incident Poynting vector calculated on the same segment (see Fig. 1). All the computations are done using a rigorous linear multiscattering theory of diffraction and an iterative scheme. More precisely, the permittivity of the rods is given by $\varepsilon_r(x,y) = \varepsilon_r^0(x,y) + \chi^{(3)}|\mathbf{E}(x,y)|^2$. For a fixed relative permittivity $\varepsilon_r(x,y)$, it is possible to compute the scattering matrix $\mathbf{S}(\lambda)$ of the

structure, linking the incident field to the diffracted one.^{19,20} This matrix may be decomposed into a linear interaction term $\mathbf{T}(\lambda)$ and a nonlinear scattering term $\mathbf{B}(\lambda)$, so that we have $\mathbf{B}(\lambda,|\mathbf{E}^d|^2)\mathbf{E}^d + \mathbf{T}(\lambda)\mathbf{E}^d = \mathbf{E}^i$. From this equation, an iterative scheme is easily derived. Starting with $\varepsilon_0(x,y) = \varepsilon_r^0(x,y)$, we compute the scattered field \mathbf{E}_0^d , and then define a sequence through

$$\varepsilon_{n+1}(x,y) = \varepsilon_n(x,y) + \chi^{(3)}|\mathbf{E}_n(x,y)|^2,$$

$$\mathbf{B}(\lambda,|\mathbf{E}_n|^2)\mathbf{E}_{n+1}^d + \mathbf{T}(\lambda)\mathbf{E}_{n+1}^d = \mathbf{E}^i, \quad (1)$$

$$\mathbf{E}_{n+1} = \mathbf{E}_{n+1}^d + \mathbf{E}^i.$$

Let us remark that the wavelength of the incident field is almost ten times bigger than the diameter *d* of the rods ($\lambda/d \sim 10$) hence the electric energy in the nonlinear rods is assumed to be constant and equal to the mean intensity

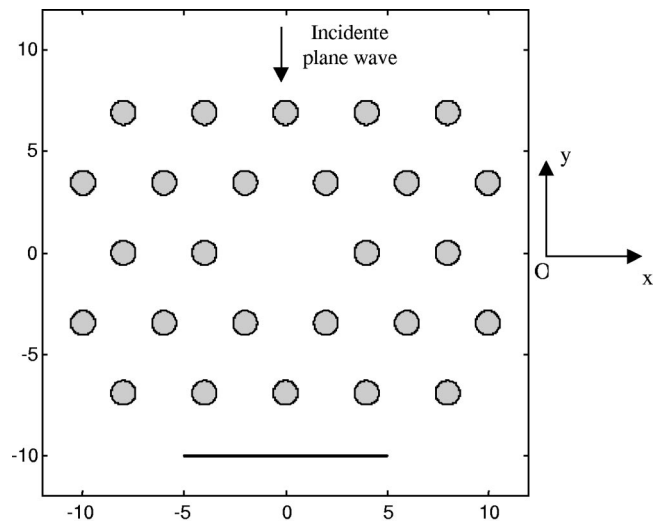


FIG. 1. 5×5 hexagonal photonic crystal doped by a microcavity. The spatial period of the lattice is $p=4$ and the diameter of the rods is $d=1$. The Kerr-type permittivity of the rods is $\varepsilon_r = \varepsilon_r^0 + \chi^{(3)}|\mathbf{E}(x,y)|^2$ with $\varepsilon_r^0 = 8.41$ and $\chi^{(3)} = -0.001$. The incident field is *s* polarized and propagates towards the negative-*y* direction. The segment below the structure is used for computation of the transmission coefficient *T*.

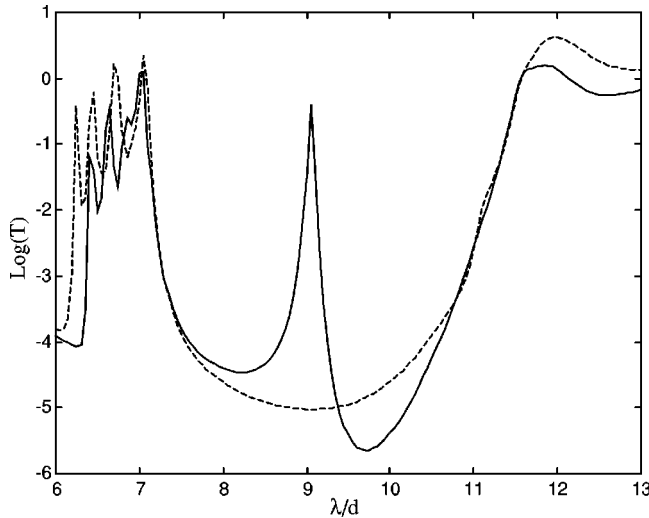


FIG. 2. Logarithm of the transmission T vs the wavelength λ for the crystal of Fig. 1 (solid curve) and for the same crystal with the central rod (dashed curve). The microcavity creates a acceptor mode for the resonant wavelength $\lambda_a/d=9.056$.

$\langle |\mathbf{E}_n(x,y)|^2 \rangle$. From a numerical point of view, it is necessary to interpolate and to replace the permittivity ε_n by $\tilde{\varepsilon}_n$ defined as:

$$\tilde{\varepsilon}_{n+1} = \varepsilon_n + f(\varepsilon_{n+1} - \varepsilon_n). \quad (2)$$

The parameter f represents a relaxation factor in the iterative process, which is chosen in the interval $(0,1)$. In all the numerical computations that we did, the number of requested iterations required to obtain a relative precision of 10^{-3} on ε_r varied from 3 to 100 with $f=0.3$.

In the first numerical experiment, all the fibers are of Kerr nonlinear type, with a negative (nonfocusing) $\chi^{(3)}$ coefficient chosen equal to -0.001 . In the case of a very weak incident field, the crystal is in the linear regime, and it exhibits a gap in the interval of wavelengths $(7,11)$. Moreover, as it is doped by a microcavity, there exists a deep acceptor mode at $\lambda_a/d=9.056$ (Fig. 2).

We study the transmission T as a function of the amplitude A of the incident field for three wavelengths shorter than that of the defect mode in the linear regime (see Fig. 3). For $\lambda/d=8.960$, we observe clearly a hysteresis loop, characteristic of bistability, allowing an optical switching through the photonic crystal: for an amplitude $A=4$, growing up to 6.9 the transmission describes the curve $\mathcal{A} \rightarrow \mathcal{B}$ (Fig. 3). At the threshold amplitude $A_t=7$ the crystal switches to a transmitting state (point \mathcal{B}') (Fig. 3). When lowering the intensity the transmission describes the curve $\mathcal{B}' \rightarrow \mathcal{D} \rightarrow \mathcal{D}' \rightarrow \mathcal{A}$. In contrast to previous studies, the switching here is made possible by the existence of a defect mode and not by the mobility of the edges of the gap. This is a very important remark, as the existence of bistability is ensured not only at the edge of the gap but on a full interval of wavelengths. Moreover it is possible to control with a fair accuracy the frequency of the defect mode.²¹ Another fundamental remark is that for finite structures the boundary of the gap is not very stiff, hence the switch of ratio of transmitted energy cannot be very high,

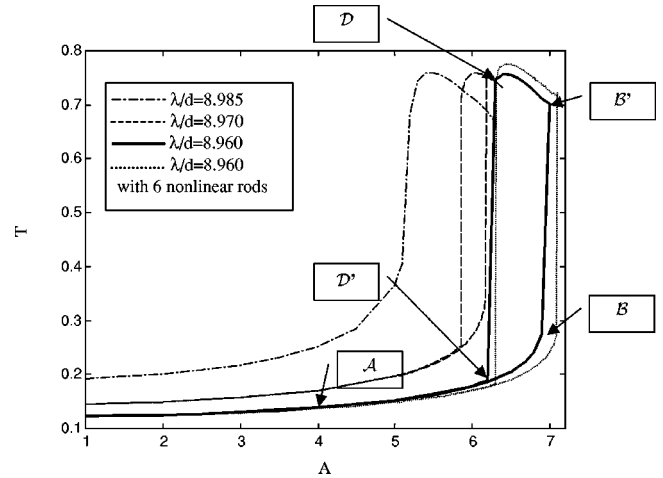


FIG. 3. Transmission T vs the amplitude A computed for three wavelengths. The bistability phenomenon occurs for wavelengths lower than $\lambda/d=8.980$ (see dashed and solid line curve). For the wavelength $\lambda/d=8.985$ the transmission switches from a nonpassing state to a propagative one (dotted-dashed curve). The dotted curve presents the transmission for the crystal with only six nonlinear rods situated on the boundary of the microcavity.

whereas in the present case, using a defect mode, the transmission is multiplied by a factor of 4.

Let us now turn to a more detailed description of the phenomena underlying bistability. In the weak field limit, the scattering matrix in the vicinity of the defect can be written as

$$\mathbf{S}(\lambda) = \frac{|\psi\rangle\langle\psi|}{\lambda - \lambda_p} + \mathbf{S}_0(\lambda); \quad (3)$$

the complex number λ_p is called a pole of the scattering operator, and the residue operator $|\psi\rangle\langle\psi|$ accounts for the resonant behavior whereas \mathbf{S}_0 accounts for the evanescent waves. The residue operator is defined through the functional integral $|\psi\rangle\langle\psi| = \int_{\gamma} \mathbf{S}(z) dz$ where γ is a loop in the complex plane containing the pole λ_p . Its range is the kernel of $\mathbf{S}^{-1}(\lambda_p)$. Therefore the residue operator is a projector on the defect mode, and the coupling between the incident field and the defect mode is proportional to $\langle\psi|\mathbf{E}^i\rangle$. Later on, this will help us in studying the influence of the source on the threshold intensity.

It is now important to note that as the defect mode is concentrated in the microcavity, it is a natural question to wonder whether it is necessary that all the rods are nonlinear ones in order to get the bistability phenomenon. Figure 4 presents the variation of the permittivity of three rods inside the crystal with respect to the intensity of the incident field: because of the strong localization of the light inside only the rods at the boundary of the microcavity have their permittivity significantly modified (the relative variation of the permittivity is higher than 8%). As a consequence, we expect bistability and switching to happen when all the rods are replaced by linear ones, except those on the boundary of the microcavity. This is what is done in the next numerical experiment (see Fig. 3), and we indeed obtain bistability and switching, with an almost unchanged threshold $A_t=7.1$. Now it is very important to note that due to the symmetry of

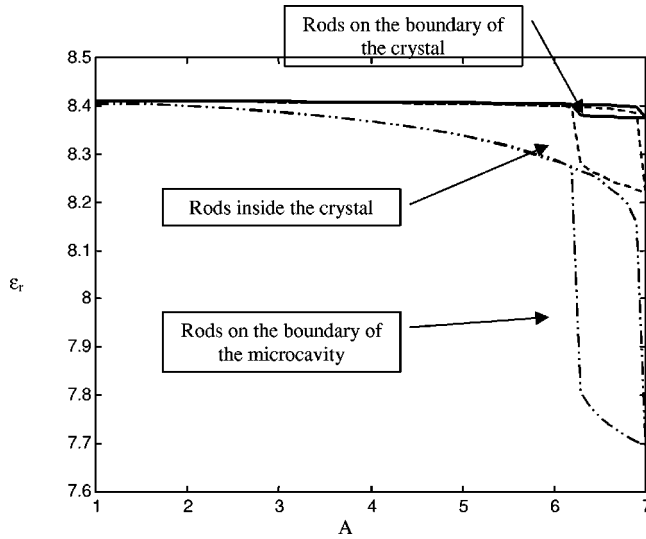


FIG. 4. Permittivity inside three rods of the crystal vs the amplitude A of the incident plane wave.

the defect mode and that of the crystal, these nonlinear rods all have the same nonlinear permittivity. That way, we have reduced our problem to simply computing the evolution of the defect mode with respect to the permittivity of the rods on the boundary of the microcavity, and thus to a family of linear problems.

We now turn back to a linear problem, where the microcavity edge rods have a varying permittivity ε_r . For each value of ε_r , we compute the value of the pole λ_p [this is done by minimizing the eigenvalue of smallest modulus of $\mathbf{S}^{-1}(\lambda)$], see Fig. 5, where it is seen that the variation of the real part of λ_p is linear: $\text{Re}(\lambda_p/d) = a\varepsilon_r + b$ with $a = 0.145$ and $b = 7.84$. The shift of the resonance is directly given by the sign of the susceptibility tensor $\chi^{(3)}$. When it is positive, the permittivity of the nonlinear rods grows and hence the value of the pole λ_p as well: this induces a red shift, i.e., towards lower energies levels, in the edges of the gaps and in the resonances. Conversely, in case of a negative $\chi^{(3)}$ there is a blue shift, i.e., towards higher energies levels. These predictions are in full agreement with previous studies on the evolution of the bandedges.^{18,22}

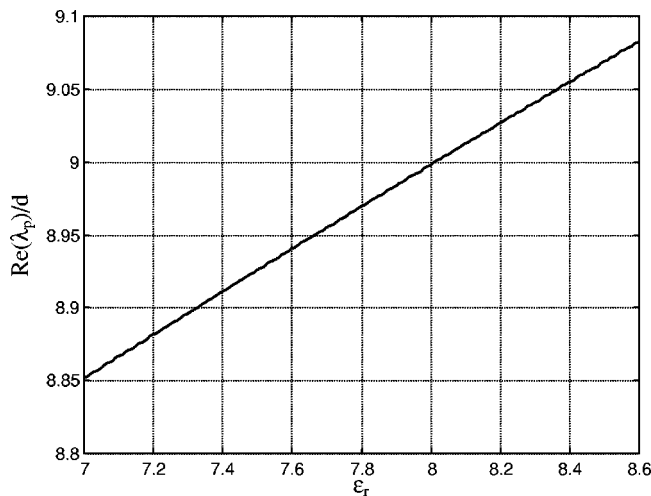


FIG. 5. Real part of the pole of the scattering operator vs the permittivity of rods situated on the boundary of the microcavity.

Let us now study the variation of the field inside the crystal at a fixed wavelength λ , when varying ε_r . The relevant quantity for the transition from the gap to the defect mode is $|\lambda - \lambda_p(\varepsilon_r)|^{-2}$, as can be seen from Eq. (3). Indeed, when $\lambda_p(\varepsilon_r)$ is far from λ then the predominant term in $\mathbf{S}(\lambda)$ is \mathbf{S}_0 whereas when $\text{Re}[\lambda_p(\varepsilon_r)]$ is in the very near vicinity of λ the predominant term is

$$\frac{|\psi\rangle\langle\psi|}{\lambda - \lambda_p(\varepsilon_r)}.$$

Therefore, as \mathbf{S}_0 represents evanescent waves, the energy of the field inside the crystal is proportional to $|\lambda - \lambda_p(\varepsilon_r)|^{-2}$. Let us denote by ε_{op} the permittivity of the rods for which the real part of the pole is equal to the wavelength [i.e., $\lambda = \text{Re}[\lambda_p(\varepsilon_{op})]$] and therefore the energy inside the rods becomes maximal

$$\langle |\mathbf{E}|_{\text{max}}^2 \rangle \propto \frac{\langle \psi | \mathbf{E}^i \rangle^2}{\text{Im}[\lambda_p(\varepsilon_{op})]^2}. \quad (4)$$

In the nonlinear case, at a given incident field $A \mathbf{E}^i$ (with amplitude A and $|\mathbf{E}^i| = 1$), we denote by $\varepsilon(A)$ the permittivity of the nonlinear rods. Then we have that the normalized amplitude of the field inside these rods is given by

$$\frac{\langle |\mathbf{E}|^2 \rangle}{\langle |\mathbf{E}|_{\text{max}}^2 \rangle} = \frac{\text{Im}[\lambda_p(\varepsilon_{op})]^2}{|\lambda - \lambda_p[\varepsilon(A)]|^2} A^2; \quad (5)$$

a second relation is obtained by the very definition of a Kerr medium: $\varepsilon_r = \varepsilon_r^0 + \chi^{(3)} \langle |\mathbf{E}|^2 \rangle$. It follows from these relations that the normalized intensity of the field inside the nonlinear rods is given by the intersection of the curve:

$$\varepsilon_r \mapsto \frac{\text{Im}[\lambda_p(\varepsilon_{op})]^2}{|\lambda - \lambda_p(\varepsilon_r)|^2}, \quad (6)$$

and the straight line

$$\varepsilon_r \mapsto \frac{\text{Im}[\lambda_p(\varepsilon_{op})]^2}{\langle \psi | \mathbf{E}^i \rangle^2} \frac{\varepsilon_r - \varepsilon_r^0}{\chi^{(3)} A^2}. \quad (7)$$

From this geometrical construction it is possible to understand and predict bistability, see Fig. 6. The qualitative behavior of the nonlinear diffraction problem is given by the intersections of the graphs of the functions defined by Eqs. (6) and (7). We start with a wavelength $\lambda/d = 8.960$ and with a small amplitude of the incident field $A = 4$. Graphically we get a unique solution \mathcal{A} . As the amplitude A grows to the value 7.1 the part $\mathcal{A} \rightarrow \mathcal{B}$ of the curve is described. For an increasing value of the amplitude A the solution jumps to the point \mathcal{B}' , this effect explains the switching between the evanescent state of the electromagnetic field and the defect mode state (see Fig. 3). For an amplitude belonging to the interval (7.1; 10) the solutions describe the curve $\mathcal{B}' \rightarrow \mathcal{C}$. When the intensity is lowered, the parts $\mathcal{C} \rightarrow \mathcal{B}'$ and $\mathcal{B}' \rightarrow \mathcal{D}$ are reached. For an amplitude lower than 6.3, the solution jumps to the point \mathcal{D}' and the part of the curve $\mathcal{D}' \rightarrow \mathcal{A}$ is described. This simple graphical analysis explains the bistability phenomenon obtained for the transmission in Fig. 3. Moreover, we can predict the amplitude of the inci-

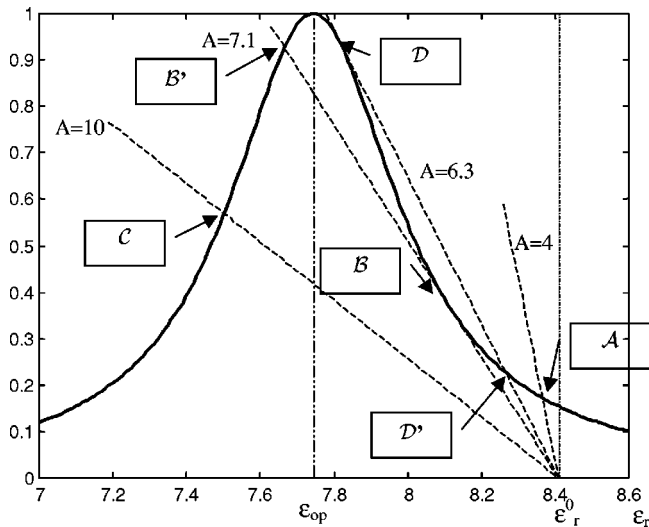


FIG. 6. The solid curve represents the function of Eq. (6) vs the permittivity. The straight line represents Eq. (7) for different amplitudes A . The intersection points give the number of solutions of the nonlinear diffraction problem as well as the corresponding parameters.

dent field necessary to obtain the switch between different states of energy: the graphical threshold is equal to 7.1 in agreement with the numerical computation of Fig. 3 ($A_t=7.1$). We can also compute the minimal detuning in order to have the bistability effect. Indeed, the bistability phenomenon occurs when for a given amplitude A there exist two intersection points. This criterion is verified for a difference $\epsilon_r^0 - \epsilon_{op}$ higher than 0.5. Using the linear relation be-

tween $\text{Re}(\lambda_p)$ and ϵ_r we determine the minimal detuning $\Delta\lambda/d = -0.07$. Hence bistability appears for wavelengths lower than $\lambda/d = 8.980$. This result is confirmed by the numerical computation of the transmission T versus the amplitude of the incident field: for $\lambda/d = 8.985$ bistability does not appear whereas for $\lambda/d = 8.970$ there exists a small hysteresis loop (see Fig. 3).

The term $\langle \psi | \mathbf{E}^i \rangle$, i.e., the coupling coefficient of the modes, is a very important quantity. Indeed, it rules the intensity threshold for obtaining bistability: the bigger it is, the smaller the amplitude should be, because the relevant quantity is the slope of the straight line (7), as explained above. For instance, at $\lambda/d = 8.960$, the threshold intensity is $A_t = 7.1$ for an incident plane wave, whereas for a wire antenna situated at the middle of the microcavity (and hence generating an incident wave with symmetry close to that of the mode), the threshold intensity is reduced by a factor of 4.

Using a rigorous multiscattering theory we have demonstrated the bistability behavior through a defect mode inside a finite-size two-dimensional photonic crystal. Thanks to a linear analysis using the determination of the poles of the scattering operator, we have derived a graphical method allowing the computation of the minimal detuning and the threshold amplitude of the incident field. We have pointed out the influence of the choice of the sources of excitation: using a wire antenna in order to optimize the coupling with the defect mode, the threshold intensity becomes minimal. In our opinion the localization properties of photons inside doped nonlinear photonic crystals may lead to new classes of active optical components. Indeed, thanks to the strong localization the electromagnetic energy is locally enhanced, which then allows strong nonlinear phenomena.

¹J. D. Joannopoulos, R. Meade, and J. Winn, *Photonic Crystals* (Princeton University Press, Princeton, N.J., 1995).
²E. Yablonovitch, *Phys. Rev. Lett.* **58**, 2059 (1987).
³S. Fan *et al.*, *Phys. Rev. Lett.* **80**, 960 (1998).
⁴E. Centeno, B. Guizal, and D. Felbacq, *Pure Appl. Opt.* **1**, L10 (1999).
⁵R. D. Meade, A. Devenyi, J. D. Joannopoulos, O. L. Alerthand, D. A. Smith, and K. Kash, *J. Appl. Phys.* **75**, 4753 (1994).
⁶E. R. Brown, C. D. Parker, and E. Yablonovitch, *J. Opt. Soc. Am. B* **10**, 404 (1993).
⁷F. Delyon, Y. E. Lévy, and B. Souillard, *Phys. Rev. Lett.* **57**, 2010 (1986).
⁸Q. Li, C. T. Chan, K. M. Ho, and C. M. Soukoulis, *Phys. Rev. B* **53**, 15 577 (1996).
⁹M. D. Tocci, M. J. Bloemer, M. Scalora, J. P. Dowling, and C. M. Bowden, *Appl. Phys. Lett.* **66**, 2324 (1995).

¹⁰M. Scalora, J. P. Dowling, C. M. Bowden, and M. J. Bloemer, *Phys. Rev. Lett.* **73**, 1368 (1994).
¹¹W. Chen and D. L. Mills, *Phys. Rev. Lett.* **58**, 160 (1987).
¹²D. L. Mills and S. E. Trullinger, *Phys. Rev. B* **36**, 947 (1987).
¹³D. N. Christodoulides and R. I. Joseph, *Phys. Rev. Lett.* **62**, 1746 (1989).
¹⁴S. John and N. Aközbeek, *Phys. Rev. Lett.* **71**, 1168 (1993).
¹⁵N. Aközbeek and S. John, *Phys. Rev. E* **57**, 2287 (1998).
¹⁶B. Xu and N. B. Ming, *Phys. Rev. Lett.* **71**, 1003 (1993).
¹⁷B. Xu and N. B. Ming, *Phys. Rev. Lett.* **71**, 3959 (1993).
¹⁸Z. L. Wang *et al.*, *Phys. Rev. B* **53**, 6984 (1996).
¹⁹E. Centeno and D. Felbacq, *J. Opt. Soc. Am. A* **16**, 2705 (1999).
²⁰G. Tayeb and D. Maystre, *J. Opt. Soc. Am. A* **14**, 3323 (1997).
²¹E. Yablonovitch *et al.*, *Phys. Rev. Lett.* **67**, 3380 (1991).
²²P. Tran, *Phys. Rev. B* **52**, 10 673 (1995).